ARTICLE

Production of Mixed Alcohols from Bio-syngas over Mo-based Catalyst

Song-bai Qiu, Wei-wei Huang, Yong Xu, Lu Liu, Quan-xin Li*

Department of Chemical Physics, Anhui Key Laboratory of Biomass Clean Energy, University of Science and Technology of China, Hefei 230026, China

(Dated: Received on August 5, 2010; Accepted on September 25, 2010)

A series of Mo-based catalysts prepared by sol-gel method using citric acid as complexant were successfully applied in the high efficient production of mixed alcohols from bio-syngas, derived from the biomass gasification. The $Cu_1Co_1Fe_1Mo_1Zn_{0.5}$-6%K catalyst exhibited a higher activity on the space-time yield of mixed alcohols, compared with the other Mo-based catalysts. The carbon conversion significantly increases with rising temperature below 340 °C, but the alcohol selectivity has an opposite trend. The maximum mixed alcohols yield derived from biomass gasification is 494.8 g/(kg_{catal}·h) with the $C2^+$ (C2−C6 higher alcohols) alcohols of 80.4% under the tested conditions. The alcohol distributions are consistent with the Schulz-Flory plots, except methanol. In the alcohols products, the $C2^+$ alcohols (higher alcohols) dominate with a weight ratio of 70%−85%. The Mo-based catalysts have been characterized by X-ray diffraction and N_2 adsorption/desorption. The clean bio-fules of mixed alcohols derived from bio-syngas with higher octane values could be used as transportation fuels or petrol additives.

Key words: Biomass, Bio-syngas, Mixed alcohol, Mo-based catalyst

I. INTRODUCTION

Increasing concerns about the increased energy demand, global climate change, depletion of fossil fuel resources, and the rise of oil prices has pushed the renewable energy such as biomass energy to the hotspot topics in recent years [1, 2]. Biomass is a rich, environmentally friendly and renewable resource which is globally available, and can be used as an alternative feedstock for energy source or chemicals [3−5]. As an only renewable carbon resource, biomass can be converted into a wide range of liquid fuels (called as bio-fuels) or chemicals based on the thermochemical and biochemical processes, including bio-oil, bio-ethanol, bio-diesel, liquid hydrocarbons (*e.g.*, gasoline, diesel, waxes), mixed alcohols, dimethyl ether (DME), acetic acid, and formaldehyde [6, 7]. So far, only two biomass-based fuels of bio-ethanol and bio-diesel have been well-developed and commercialized for production [7]. However, most of the materials used for production bio-ethanol and bio-diesel are edible matters with the selected and limited biomass feedstocks in the real application. In addition, the raw bio-oil from various biomass by pyrolysis processes can not be directly used in gasoline or diesel engines because of low heating value, poor volatility, high viscosity, coking, corrosiveness, and high water content, and it must be upgraded prior to being used as a replacement for diesel and gasoline fuels [8].

In principle, biomass can be thermochemically converted to bio-syngas through biomass gasification or bio-oil reforming process [9, 10]. Bio-syngas can be further catalytically synthesized into various bio-fuels and chemicals, especially to methanol, ethanol, mixed alcohols and FT (Fischer-Tropsch) fuels. The unstinted feedstock type of biomass, such as cellulose, hemicellulose and lignin, is one major advantage of this synthesis route [2, 11, 12].

With stringent restrictions on pollution emissions, alcohols appear to be not only environmentally friendly fuel additives, but also effective as potential octane number enhancer for motor fuels. Although methanol would provide some advantages as mixed alcohols, it has many disadvantages such as phase separation caused by limited miscibility between methanol and gasoline, corrosion of metals, plastics and elastomers associated with the use of methanol in fuel systems [13, 14]. As a potential alternative fuel/additive or chemical raw materials, the higher alcohols (C1−C6 mixed alcohols) have many advantages including complete combustion, higher octane numbers, volatility control, lower toxic exhaust gas (CO, NO_x) emissions, excellent substitutes for methyl tert-butyl ether (MTBE), and higher product added value [15, 16]. So the catalytic conversion of synthesis gas to mixed alcohols is now attracting renewed attention for both industrial application and fundamental research.

A wide range of homogeneous and heterogeneous catalysts have been explored and well reviewed in Ref.[17]. Briefly, the catalysts employed in the synthesis of

*Author to whom correspondence should be addressed. E-mail: liqx@ustc.edu.cn

ethanol and mixture alcohols from the hydrogenation of CO can be broadly classified into four types: (i) noble metals-based synthesis catalysts, (ii) modified methanol synthesis catalysts, (iii) modified Fischer-Tropsch synthesis catalysts, and (iv) Mo-based synthesis catalysts.

The noble metals-based catalysts are primarily focused on rhodium (Rh) catalysts [2]. Although Rh-based catalysts exhibit a higher selectivity to ethanol or $C2^+$-oxygenates, the commercial availability of these catalysts seems strongly limited because of exorbitant prices. The modified methanol synthesis catalysts based on Cu-ZnO/Al_2O_3 or ZnO/Cr_2O_3 with various alkali promoters such as Li, Na, K and Cs, Pd promoter, Fe-modifier *etc.* [18], have also been explored. The modified methanol synthesis catalysts generate less byproduct of hydrocarbons, but these catalysts also show lower yield to $C2^+$-alcohols. The modified Fischer-Tropsch synthesis catalysts generally contain Co, Fe, Ni, or Ru metals (*i.e.*, FT elements) together with a wide range of metal promoters (Cu, Mo, Mn, Re, Ru *etc.*), alkali promoters (Li, K, Cs *etc.*), and supporters (SiO_2 or Al_2O_3 *etc.*) [19]. The modified FT synthesis catalysts generally favor to produce relatively higher yields of high alcohols ($C2^+$-alcohols), typically ranging from 100 mg to 500 mg $C2^+$-alcohols/(g_{catal}·h), accompanying a significant amount of hydrocarbons.

The Mo-based catalysts such as Mo carbide, Mo sulfide, and Mo oxide with various alkali promoters (K and Cs) and metal promoters (Ni, Rh, and Co) [20] have also been developed for high alcohols synthesis. Compared with other catalysts, the Mo-based catalysts are more attractive for commercial aspects due to their excellent resistance to sulfur poisoning and high activity for water gas shift reaction, which would save the considerable costs of ultra-desulfurization for feed gas and separation of water. However, the alcohol yield over these Mo-based catalysts is lower than that over the CuCo-based catalysts. And the operating pressure (5.5−13.8 MPa) seems obviously higher than that of modified methanol synthesis catalysts or modified FT type catalysts. Moreover, the preparations for these Mo-based catalysts need sulfuration or carbonization. The Mo-based catalysts are facing major challenges in improving catalytic activity, reducing operating pressure, and simplifying the catalyst preparation methods.

In our previous work, attention has been paid to producing syngas from the biomass gasification and the bio-oil reforming, both in lab and pilot plant scales [21−25]. In this work, we aims to efficiently produce mixed alcohols over the Mo-based catalysts from the biomass gasification (BGS). Especially, the study of the biomass-based mixed alcohols synthesis placed emphasis on improvement of the Mo-based catalysts, enhancing the catalytic activity, increasing the yield of synthesis, optimizing the reaction conditions. Biomass gasification-synthesis route could produce mixed alcohols through the use of any biomass resource in large quantities. However, the biomass-based syngas conversion to mixed alcohols remains challenging, and no commercial process exists so far although there is a growing worldwide interest in this topic for the past decades. Further researches and developments in catalyst and processing need to be achieved to make this conversion commercially attractive.

II. EXPERIMENTS

A. Catalyst preparation and characterization

The Mo-based mixture oxide catalysts with a settled molar ratio were prepared by the sol-gel method (Co/Mo molar ratio is 0.5) [26]. The preparation of catalysts is as follows: firstly, metal nitrates and $(NH_4)_6Mo_7O_{24}$ (AR) aqueous solutions were prepared with certain deionized water respectively and citric acid (molar ratio of citric acid to total metallic ions is 0.4) was added to the metal nitrate solutions under constant ultrasound dissolving, and then slowly mixed two solutions. Finally, K_2CO_3 solution was dropped slowly into the above solution. After ultrasound oscillating for another 2 h, the solution was kept in a drying oven at 90 °C until the solution released lots of bubbles. Then, the solution was immediately transferred into a muffle furnace at 350 °C and kept in air for 1 h. Soon after, the fluffy precursor was calcined at 450 °C for 3 h in air to obtain the corresponding mixture oxide catalysts. The mixture oxide catalysts were finally crushed into 40−60 mesh for the mixed alcohols synthesis.

The contents of the metal oxides in the catalysts prepared were measured by inductively coupled plasma and atomic emission spectroscopy (ICP/AES, Atom scan Advantage of Thermo Jarrell Ash Corporation, USA). The Brunauer-Emmett-Teller (BET) surface area and pore volume was determined by the N_2 physisorption at −196 °C using a COULTER SA 3100 analyzer. X-ray diffraction (XRD) patterns for the fresh and reduced catalysts were measured by an X'pert Pro Philips diffractrometer, using a Cu Kα radiation (λ=0.1541841 nm). The measurement conditions were in the 2θ=20°−80°, step counting time of 5 s, and step size of 0.017° at 298 K.

B. Reaction system for mixed alcohols synthesis

The performance of mixed alcohols synthesis from the selected BGS over the different Mo-based catalysts was evaluated in a fixed-bed continuous-flow reactor using an on-line gas chromatograph (GC) detection system (Fig.1). Usually, 1.0 g catalyst, diluted with a 2.0 mL Pyrex beads, was used for each test. Before the synthesis reactions, the catalysts were reduced in flowing H_2 with a stepwise reduction procedure up to 450 °C for 20 h. Then, the syngas was conducted to the reactor for the mixed alcohols syn-

DOI:10.1088/1674-0068/24/01/77-84

TABLE I Catalytic screening and distribution of alcohols for mixed alcohol synthesis from the BGS (T=320 °C, P=6.0 MPa, and GHSV=7.500 L/(g·h)).

Catalysts	$[CO]_{conv}$	S/%		STY(Alc.)/(g/(kg·h))	Alcohols distribution/%						
		Alc.	Hc.		C1	C2	C3	C4	C5	C6	$C2^+$
Co_1Mo_2-2%K	5.8	46.2	53.8	29.1	43.4	31.8	15.2	5.9	2.6	1.1	56.6
$Co_1Fe_1Mo_2$-2%K	7.4	67.6	32.4	45.6	26.4	38.8	17.4	8.5	5.6	3.3	73.6
$Cu_1Co_1Fe_1Mo_2$-2%K	39.4	46.1	53.9	210.6	27.7	32.3	21.7	10.4	5.2	2.7	72.3
$Cu_1Co_1Fe_1Mo_2Zn_{0.5}$-2%K	28.3	54.6	45.4	164.8	27.8	37.3	18.6	8.9	4.6	2.8	72.2
$Cu_1Co_1Fe_1Mo_1Zn_{0.5}$-2%K	54.1	45.0	55.0	257.3	30.8	31.1	22.5	9.5	4.1	2.0	69.2
$Cu_1Co_1Fe_1Mo_1Zn_{0.5}$-6%K	45.9	53.6	46.4	269.2	18.2	39.5	20.1	11.3	6.9	4.0	81.8

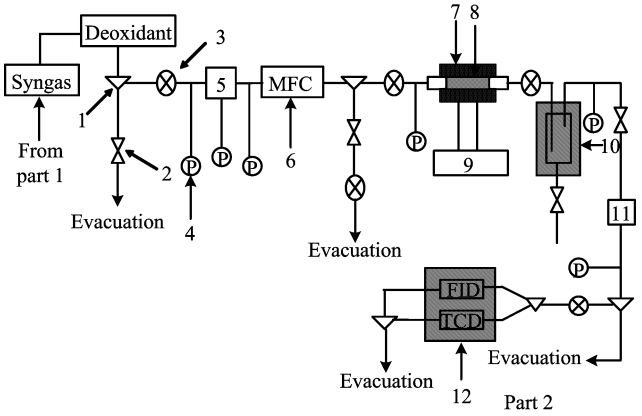

FIG. 1 Schematic setup of the fixed-bed flow reaction system for mixed alcohols synthesis. 1. Tripletee valve, 2. shut off valve, 3. micrometering valve, 4. pressure indicator, 5. pressure controller, 6. mass flow controller, 7. furnace, 8. reactor, 9. temperature controller, 10. condenser, 11. counterbalance valve, and 12. gas chromatography.

thesis under a setup synthesis condition. The synthesis was carried out under the following operating conditions: T=300−340 °C, P=6.0 MPa, GHSV (gas hourly space velocity)=7.5−15 L/(g·h). Products were quantitatively analyzed by two gas chromatographs systems on line every 30−60 min. The gases of H_2, CO, N_2, and CO_2 were detected by GC1 (Model: SP6890, column: TDX-01) with a thermal conductivity detector (TCD), using ultrahigh purity argon (99.999%) as carrier gas and gas hydrocarbons were detected by GC2 (Model: SP6890, column: Porapark-Q, USA) with a flame ionization detector (FID). The condensable vapors (mainly consisting of mixed alcohols and water) were cooled into a liquid tank and then detected off line by GC2 with a FID. The performance of mixed alcohols synthesis was evaluated by the carbon conversion $[C]_{conv}$, space time yield of mixed alcohols (STY(Alc.)), selectivity of alcohols ($S_{Alc.}$), and hydrocarbons ($S_{Hc.}$), according to the following equations [27, 28]:

$$[C]_{conv} = \frac{x_{inCO} - x_{outCO}}{x_{inCO}} \times 100\% \quad (1)$$

$$STY(Alc.) = \frac{M_{Alc.}}{M_{cata.}t} \quad (2)$$

$$S_{Alc.} = \frac{x_{Alc.}}{x_{Alc.} + x_{Hc.}} \times 100\% \quad (3)$$

$$S_{Hc.} = \frac{x_{Hc.}}{x_{Alc.} + x_{Hc.}} \times 100\% \quad (4)$$

where x_{inCO}, x_{outCO}, $x_{Alc.}$, and $x_{Hc.}$ are the carbon moles of CO_{in}, CO_{out}, alcohols, and hydrocarbons, respectively; $M_{Alc.}$ and $M_{cata.}$ are weigh of alcohols and catalyst; and t is reaction time. $S_{Alc.}$ and $S_{Hc.}$ were calculated on a CO_2 free basis.

III. RESULTS AND DISCUSSION

A. Feedstock for mixed alcohols synthesis

In this work, one bio-syngas derived from BGS was used for the mixed alcohols synthesis. The main components of bio-syngas include H_2, CO, CO_2, N_2, CH_4, and others with contents of 62.80%, 30.89%, 2.96%, 1.75%, 1.20%, and 0.40%, respectively [29]. The BGS was produced by biomass gasification in a circulating fluidized bed using rice husks with the gasification temperature of 1000−1300 °C and pressure of 1.5−3.0 MPa, followed by conditioning the syngas via WGS and purification processes [29].

B. Conversion of BGS to mixed alcohols

Table I show the performance of the mixed alcohols synthesis using BGS over the Mo-based catalysts modified by multielements under the synthesis conditions: T=320 °C, P=6.0 MPa and GHSV=7.5 L/(g·h). While adding Fe element to the Co_1Mo_2-2%K catalyst, the activity of the $Co_1Fe_1Mo_2$-2%K catalyst slightly ascends, and $C2^+$ alcohols greatly increase from 56.6% to 73.6% in the alcohols products. This indicates that the Fe element in the catalyst favors to produce higher alcohols. Adding the promoter of Cu to the $Co_1Fe_1Mo_2$-2%K synthesis catalysts conduces to significantly enhance the catalytic activity with the carbon conversion increasing from 7.4% to 39.4%. Sequen-

DOI:10.1088/1674-0068/24/01/77-84

TABLE II Performance of mixed alcohol synthesis using the BGS over the $Cu_1Co_1Fe_1Mo_1Zn_{0.5}$-6%K catalyst under the synthesis conditions: T=300−340 °C, P=6.0 MPa.

T/°C	$[CO]_{conv}$	S/%		STY(Alc.)/(g/(kg·h))	Alcohols distribution/%						
		Alc.	Hc.		C1	C2	C3	C4	C5	C6	$C2^+$
300[a]	25.4	59.2	40.8	150.3	24.2	35.3	18.8	10.6	7.4	3.7	75.8
320[a]	45.9	53.6	46.4	269.2	18.2	39.5	20.1	11.3	6.9	4.0	81.8
330[a]	52.7	51.4	48.6	286.6	17.1	42.5	21.1	10.0	5.9	3.4	82.9
340[a]	59.2	41.3	58.7	257.5	15.5	45.7	21.5	9.9	4.9	2.5	84.5
330[b]	39.4	55.6	44.4	494.8	19.6	40.4	20.7	11.3	5.2	2.8	80.4

[a] GHSV=7.5 L/(g·h).
[b] GHSV=15 L/(g·h).

tially appending Zn to $Cu_1Co_1Fe_1Mo_2$-2%K, the activity of the $Cu_1Co_1Fe_1Mo_2Zn_{0.5}$-2%K is restrained, but the selectivity of mixed alcohols increases from 46.1% to 54.6%. The superfluous amount of Mo and K in the CuCoFeMoZnK catalyst suppresses the catalytic activity, but improves the selectivity of mixed alcohols obviously. The carbon conversion and space time yield almost doubles when the content of Mo element in the CuCoFeMoZnK catalyst reduces nearly by half. More K added to $Cu_1Co_1Fe_1Mo_1Zn_{0.5}$-2%K leads to a decrease of the carbon conversion from 54.1% to 45.9%, accompanying with a certain increase of the alcohols yield and $C2^+$ alcohols. The maximum STY of mixed alcohols 269.2 g/(kg·h) was obtained over $Cu_1Co_1Fe_1Mo_1Zn_{0.5}$-6%K catalyst within the tested conditions.

C. Influence of operating conditions on mixed alcohols synthesis

Table II shows the influence of operating conditions (temperature and GHSV) on the mixed alcohols synthesis using BGS over the $Cu_1Co_1Fe_1Mo_1Zn_{0.5}$-6%K catalyst under the synthesis conditions with P=6.0 MPa. Commonly, temperature is one of the most critical reaction parameters in the mixed alcohols synthesis, which significantly affects the rate of kinetically controlled synthesis reactions. In the lower temperature region, an increasing temperature is conducive to the dissociative adsorption of CO and H_2 while promoting the formation of the specified intermediates (*e.g.*, alkyls and formyl species) [30, 31], which leads to an increase of the CO hydrogenation. However, another important characteristic of mixed alcohols synthesis is the unavoidable production of a large amount of hydrocarbons, and exorbitant temperature will greatly decrease the alcohols selectivity and affect the mixed alcohols STY [32, 33]. Consequently, to maximize the mixed alcohols yield, an appropriate temperature needs to be determined through experimentation and then being closely controlled at this value in the reactor.

As shown in Table II, the carbon conversion significantly increases from 25.4% to 59.2% with a rising temperature from 300 °C to 340 °C. An increasing trend is also observed for the STY of mixed alcohols during 300−330 °C, giving a maximum value of 286.6 g/(kg_{catal}·h) around 330 °C, nevertheless the yield decreases as temperature further increases over 330 °C. The selectivity towards total alcohols (C1−C6 alcohols) decreases from 59.2% to 41.3% (molar ratio) with a rising temperature versus an opposite trend for the hydrocarbons selectivity. In the hydrocarbons distribution, products are almost C1−C4 gaseous hydrocarbons besides a small quantity of liquid hydrocarbons. In the alcohols products, the $C2^+$ alcohols (C2−C6 higher alcohols) dominate with a weight percent ratio of 75.8%−84.5% and main alcohols products are methanol, ethanol, and propanol, especially ethanol is the dominant product in the total alcohols and its content can reach 30%−50% under the tested synthesis conditions. On the other hand, GHSV is another important factor which influences the mixed alcohols synthesis. The negative impact of GHSV on the carbon conversion may result from shortening residual time in the catalyst bed, while the positive impact on the fuels yield can arise from the increase of the turnover frequency of the synthesis products with increasing GHSV [34]. In contrast with temperature, the carbon conversion decreases with the increasing GHSV, accompanied by an increase of STY (biofuels). The maximum mixed alcohols yield got from BGS is about 494.8 g/(kg_{catal}·h) with the alcohols selectivity of 55.6% (molar ratio) and $C2^+$ alcohols distribution of 80.4% within our studied range.

Apart from the alcohols and hydrocarbons products, a small amount of other compounds including aldehydes, ketones, esters, and ethers were also detected.

D. Characterization of catalysts

Basic physical and chemical properties of catalysts were investigated by XRD, the BET surface area, and pore volumes. Figure 2 shows the XRD patterns of different Mo-based catalysts, which indicates several phases formed in the catalysts preparation.

DOI:10.1088/1674-0068/24/01/77-84

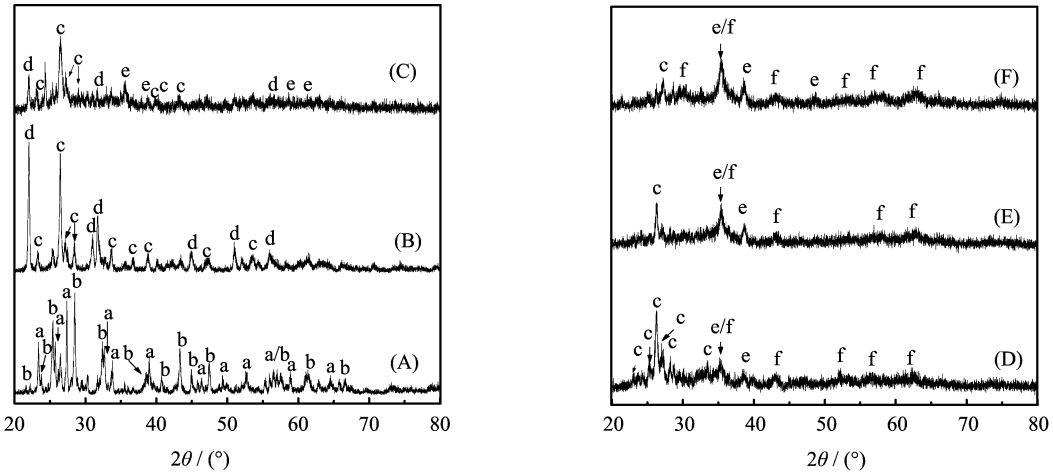

FIG. 2 The XRD patterns of Mo-based catalysts. (A) Co_1Mo_2-2%K, (B) $Co_1Fe_1Mo_2$-2%K, (C) $Cu_1Co_1Fe_1Mo_2$-2%K, (D) $Cu_1Co_1Fe_1Mo_2Zn_{0.5}$-2%K, (E) $Cu_1Co_1Fe_1Mo_1Zn_{0.5}$-2%K, (F) $Cu_1Co_1Fe_1Mo_1Zn_{0.5}$-6%K. a. MoO_3, b. $CoMoO_4$, c. $Co_{0.7}Fe_{0.3}(MoO_4)$, d. $KFe(MoO_4)_2$, e. CuO, and f. $ZnFe_2O_4$.

For Co_1Mo_2-2%K sample, the diffraction peaks can be assigned to MoO_3 and $CoMoO_4$ (PDF-05-0508 and 25-1434 cards (International Centre for Diffraction Data (ICDD)), 2002). It is considered that the new phase of MoO_3 can be formed by decomposition of $(NH_4)_6Mo_7O_{24}$ and the interaction between Co and Mo compounds can produce a new species of $CoMoO_4$. Apparently, the remarkable changes of morphology and structure are caused by the addition of Fe element. For $Co_1Fe_1Mo_2$-2%K sample, the main characteristic peaks are identified as the diffractions of $Co_{0.7}Fe_{0.3}MoO_4$ and $KFe(MoO_4)_2$ (PDF-89-6590 and 74-2010 cards). The diffraction peaks of $Cu_1Co_1Fe_1Mo_2$-2%K are similar to that of $Co_1Fe_1Mo_2$-2%K except CuO phase, but the intensities are much lower and more dispersive, indicating a smaller crystallite sizes. It is worth noting that the XRD patterns of $Cu_1Co_1Fe_1Mo_2Zn_{0.5}$-2%K are different from those of $Cu_1Co_1Fe_1Mo_2$-2%K. The diffraction peaks of $KFe(MoO_4)_2$ disappears and the very weak broad new peaks of $ZnFe_2O_4$ (PDF-22-1012 card) are detected on the sample. The intensity of the diffraction peaks for $Co_{0.7}Fe_{0.3}(MoO_4)$ phase in the $Cu_1Co_1Fe_1Mo_1Zn_{0.5}$-2%K and $Cu_1Co_1Fe_1Mo_1Zn_{0.5}$-6%K samples decreases with the Mo element content decreasing and the K element increasing, respectively. In all cases, the diffraction indicates the poorly crystalline structure. Moreover, catalysts with small crystallite sizes have an advantage to produce more alcohols while larger crystallites to methane [35, 36]. As shown in Table III, the Mo-based catalysts exhibit relatively low BET surface areas and pore volumes. The excessive content of Mo element in the catalysts leads to an obviously decrease of BET surface area and pore volume, while the Zn addition is beneficial to an increase of BET surface area.

TABLE III The BET and pore volume of Mo-based catalysts.

Catalyst	S_{BET}[a]/(m^2/g)	V_P[a]/(cm^3/g)
$Cu_1Co_1Fe_1Mo_2$-2%K	7.21	0.048
$Cu_1Co_1Fe_1Mo_2Zn_{0.5}$-2%K	11.69	0.049
$Cu_1Co_1Fe_1Mo_1Zn_{0.5}$-6%K	27.58	0.160

[a] Evaluated from the N_2 adsorption-desorption isotherms.

E. Mechanism and evaluation of biofuel synthesis

1. Roles of various compositions in Mo-based catalysts

The $Cu_1Co_1Fe_1Mo_1Zn_{0.5}$-6%K catalyst may be one of the most suitable candidates for the mixed alcohols synthesis because this non-noble metal catalyst can efficiently produce higher alcohols through CO hydrogenation. As shown in Tables I and II, the $Cu_1Co_1Fe_1Mo_1Zn_{0.5}$-6%K catalyst favors to produce fairly high yields of mixed alcohols and higher alcohols ($C2^+$-alcohols), reaching maximum yields of 0.49 kg mixed alcohols/(kg_{catal}·h) and 0.40 kg $C2^+$-alcohols/(kg_{catal}·h), respectively. In the CuCoFeMoZnK systems, Co and Fe are well known as FT synthesis elements and play important roles in the carbon chain-growth [17, 37], which lead to an increasing selectivity to the $C2^+$-alcohols, especially the selectivity to ethanol. Adding the promoters of Cu and Zn to the CuCoFeMoZnK synthesis catalysts favors to enhance the alcohols-formation [38, 39]. In the Mo-based catalysts, the added alkali has been found to be required for the alcohols-formation, which is commonly used for suppressing the hydrocarbons generation [40]. In CO hydrogenation reactions, it is generally believed that the CO molecules associatively adsorbed favor the for-

DOI:10.1088/1674-0068/24/01/77-84

mation of alcohols [15, 41]. Adding alkali to the synthesis catalysts may reduce the activity of the CO dissociative adsorption by blocking the active sites, thereby decreasing the interaction between CO and the catalyst surface, and increasing the associatively adsorbed CO hydrogenation to alcohols.

2. Formation of alcohols through CO hydrogenation

Bio-syngas derived from the biomass gasification contains a certain amount of CO and CO_2, which can be provided as a carbon source for the mixed alcohols synthesis. For the hydrogenation of CO, a generally accepted mechanism of the alcohols formation over Mo-based catalysts is "the CO insertion mechanism" [2, 17, 42]. In this mechanism, adsorbed formyl species (HC=O(a)) and adsorbed alkyl species (CH_x(a)) can be first formed from the associative or dissociative adsorption of CO and H_2 (step 1).

Step 1 (formation of HC=O(a) and CH_x(a)):

$$H_2(g) \rightarrow 2H(a) \quad (5)$$

$$CO(a) + H(a) \rightarrow HC = O(a) \quad (6)$$

$$HCO(a) + (x+1)H(a) \rightarrow CH_x(a) + H_2O \quad (7)$$

$$CO(g) \rightarrow C(a) + O(a) \quad (8)$$

$$C(a) + xH(a) \rightarrow CH_x(a) \quad (9)$$

Then, the adsorbed formyl species can react with another adsorbed H(a) species to produce methanol (step-2).

Step 2 (formation of methanol):

$$HCO(a) + 3H(a) \rightarrow CH_3OH \quad (10)$$

In addition, the adsorbed CO(a) can insert to the alkyl species CH_x(a) and form adsorbed acetyl species ($H_xC{-}C{=}O(a)$), followed by adding the H(a) species to produce ethanol (step 3).

Step 3 (formation of ethanol):

$$CO(a) + CH_x(a) \rightarrow H_xC - C = O(a) \quad (11)$$

$$H_xC - C = O(a) + (6-x)H(a) \rightarrow C_2H_5OH \quad (12)$$

Furthermore, the adsorbed CO(a) can insert to the higher carbon-numbers' alkyl species C_nH_x(a) which are generated through the chain-growth step and form adsorbed intermediate species ($C_nH_x{-}C{=}O(a)$), followed by adding the H(a) species to produce the $C_3{}^+$ alcohols (step 4).

Step 4 (formation of $C_3{}^+$ alcohols):

$$CH_x(a) + (n{-}1)C(a) \rightarrow C_nH_x(a) \quad (13)$$

$$CO(a) + C_nH_x(a) \rightarrow C_nH_x - C = O(a) \quad (14)$$

$$C_nH_x\text{-}C = O(a) + (2n{+}4{-}x)H(a) \rightarrow C_{n+1}H_{2n+3}OH \quad (15)$$

where Eq.(13), Eq.(14), and Eq.(15) are chain-growth, CO insertion, and adding H(a). The selectivities of various alcohols can be predicted based on simple statistical distributions calculated from chain growth probability and carbon number. The chain polymerization kinetics model, well known as the Anderson-Shulz-Flory (ASF) model, is represented by the following equation [43−45]:

$$\ln\frac{W_n}{n} = n\ln\alpha + \ln\frac{(1-\alpha)^2}{\alpha} \quad (16)$$

here W_n is the weight percent of a product containing n carbon atoms and α is the chain growth probability. This equation is graphically represented in Fig.3. It clearly displays the alcohols distributions, observed from the rich-CO BGS over the different Mo-based catalysts. These alcohols distributions are consistent with the Schulz-Flory equation very well, sometimes except for methanol formation deviated far from the SF plots. Compared with the traditional linear SF distribution over the Co_1Mo_2-2%K catalyst, a certainly deviation of ethanol, derived from the slope of the SF plot, was observed over the $Co_1Fe_1Mo_2$-2%K catalyst, and the alcohols chain growth probability is α=0.327±0.005 and α=0.438±0.025, respectively. This indicates that the Fe promoter exerted an effective function on the whole chain propagation to produce alcohols, especially exhibits a promotion effect on the chain propagation for the step of C1 to C2 based on the classical CO insertion mechanism [46, 47]. Adding the active elements of Cu and Zn for conventional methanol catalysts and decreasing the Mo content in the Mo-based catalyst results in a gradual decrease of value from 0.438±0.025 to 0.374±0.014. When doped by more potassium, the chain-growth probability α increases to 0.434±0.019, which suggests that more potassium promoter is conducive to the CO molecules associatively adsorbed so as to favor the alcohols formation [48].

IV. CONCLUSION

This work reports that mixed alcohols can be efficiently produced from bio-syngas, derived from BGS. A series of Mo-based catalysts were prepared by sol-gel method using citric acid as complexant and the performances of higher alcohol synthesis catalysts were investigated under the conditions: T=300−340 °C, P=6.0 MPa and GHSV=7.5−15 L/(g·h). Compared with the other Mo-based catalysts, the $Cu_1Co_1Fe_1Mo_1Zn_{0.5}$-6%K catalyst has a higher space-time yield of mixed alcohols 269.2 g/(kg·h). The optimum temperature is about 330 °C based on the mixed alcohols STY. The maximum mixed alcohols yield got from BGS is about 494.8 g/(kg_{catal}·h) with the alcohols selectivity of 55.6% (molar ratio) and $C2^+$ alcohols distribution of 80.4% within the tested conditions. In the alcohols products, the $C2^+$ alcohols (C2−C6 higher alcohols) dominate

DOI:10.1088/1674-0068/24/01/77-84

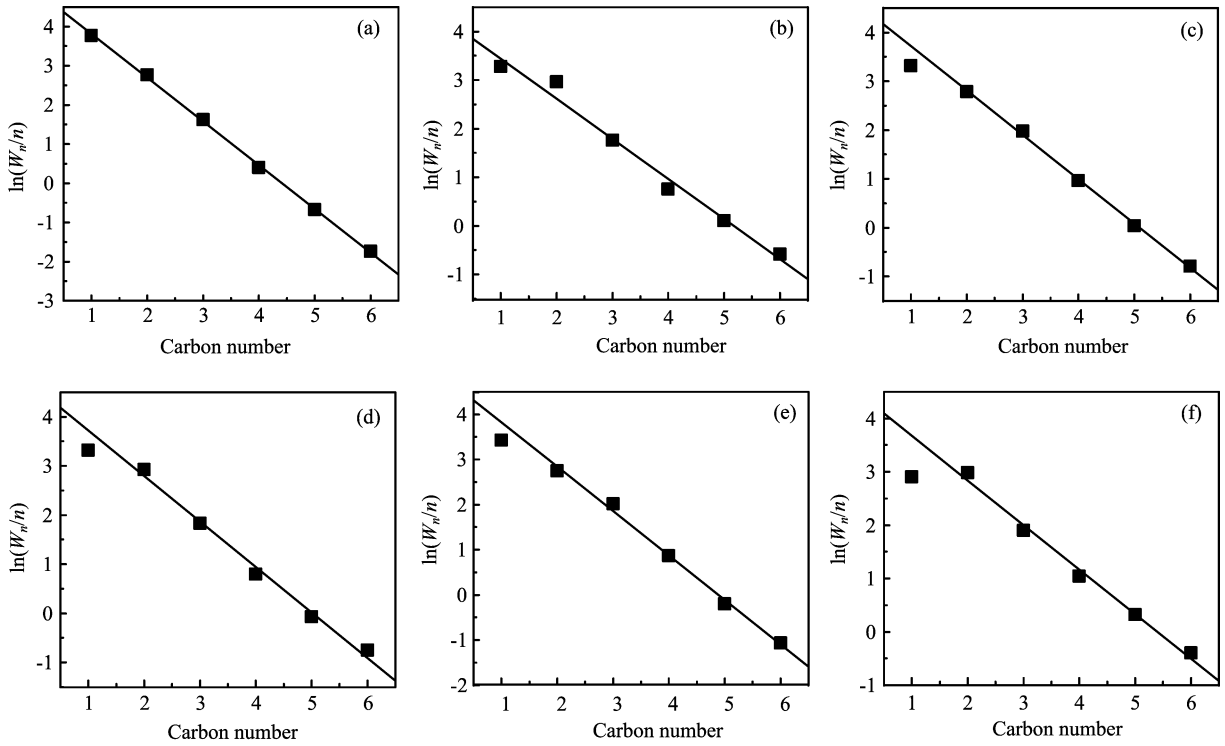

FIG. 3 Schulz-Flory plots of alcohols over Mo-based catalysts. (a) Co_1Mo_2-2%K, (b) $Co_1Fe_1Mo_2$-2%K, (c) $Cu_1Co_1Fe_1Mo_2$-2%K, (d) $Cu_1Co_1Fe_1Mo_2Zn_{0.5}$-2%K, (e) $Cu_1Co_1Fe_1Mo_1Zn_{0.5}$-2%K, (f) $Cu_1Co_1Fe_1Mo_1Zn_{0.5}$-6%K.

with a weight percent ratio of 70%−85% and main alcohols products are methanol, ethanol, and propanol, especially ethanol is the dominant product and its content can reach 30%−50% in the total alcohols. At the same time, the morphologies and structures of Mo-based catalysts modified by multielements have been characterized by XRD and BET. The active catalysts have poorly crystalline structures which indicate these catalysts possess small crystallite sizes, moreover exhibit relatively high BET surface areas and pore volumes.

The $Cu_1Co_1Fe_1Mo_1Zn_{0.5}$-6%K catalyst may be one of the most suitable candidates for the mixed alcohols synthesis from rich-CO bio-syngas because this non-noble metal catalyst can efficiently produce higher alcohols through the hydrogenation of CO. The clean biofules of mixed alcohols derived from bio-syngas with higher octane values could be used as transportation fuels or petrol additives. The bio-fuels synthesis is unstinted by the feedstocks of biomass, and potentially, may be one promising route to produce bio-fuels in future.

V. ACKNOWLEDGMENTS

This work is supported by the National High Technical Research and Development Program (No.2009AA05Z435), the National Basic Research Program of Ministry of Science and Technology of China (No.2007CB210206), and the National Natural Science Foundation of China (No.50772107).

[1] R. M. Navarro, M. A. Pena, and J. L. G. Fierro, Chem. Rev. **107**, 3952 (2007).
[2] J. J. Spivey and A. Egbebi, Chem. Soc. Rev. **36**, 1514 (2007).
[3] G. W. Huber, J. W. Shabaker, and J. A. Dumesic, Science **300**, 2075 (2003).
[4] E. Chornet and S. Czernik, Nature **418**, 928 (2002).
[5] R. D. Cortright, R. R. Davda, and J. A. Dumesic, Nature **418**, 964 (2002).
[6] L. Petrus and M. A. Noordermeer, Green Chem. **8**, 861 (2006).
[7] S. N. Naik, V. V. Goud, P. K. Rout, and A. K. Dalai, Renewable Sustainable Energy Rev. **14**, 578 (2010).
[8] S. Czernik and A. V. Bridgwater, Energy Fuels **18**, 590 (2004).
[9] P. N. Kechagiopoulos, S. S. Voutetakis, A. A. Lemonidou, and I. A. Vasalos, Ind. Eng. Chem. Res. **48**, 1400 (2009).
[10] A. A. Iordanidis, P.N. Kechagiopoulos, S.S. Voutetakis, A.A. Lemonidou, and I. A. Vasalos, Int. J. Hydrogen Energy **31**, 1058 (2006).
[11] M. J. A. Tijmensen, A. P. C. Faaij, C. N. Hamelinck, and M. R. M. van Hardeveld, Biomass Bioenergy **23**, 129 (2002).

DOI:10.1088/1674-0068/24/01/77-84

[12] E. V. Steen and M. Claeys, Chem. Eng. Technol. **31**, 655 (2008).
[13] S. A. Hedrick, S. S. C. Chuang, A. Pant, and A. G. Dastidar, Catal. Today **55**, 247 (2000).
[14] A. Muramatsu, T. Tatsumi, and H. Tominaga, J. Phys. Chem. **96**, 1334 (1992).
[15] X. D. Xu, E. B. M. Doesburg, and J. J. F. Sckolen, Catal. Today **2**, 125 (1987).
[16] A. N. Verkerk, B. Jaeger, C. H. Finkeldei, and W. Keim, Appl. Catal. **186**, 407 (1999).
[17] V. Subramani and S. K. Gangwal, Energy Fuels **22**, 814 (2008).
[18] M. Xu and E. Iglesia, J. Catal. **188**, 125 (1999).
[19] M. A. Fraga and E. Jordao, React. Kinet. Catal. Lett. **64**, 331 (1998).
[20] V. R. Surisetty, A. K. Dalai, and J. Kozinski, Ind. Eng. Chem. Res. (2010).
[21] T. Kan, J. Xiong, X. Li, T. Ye, L. Yuan, Y. Torimoto, M. Yamamoto, and Q. Li, Int. J. Hydrogen Energy **35**, 518 (2010).
[22] L. Yuan, Y. Chen, C. Song, T. Ye, Q. Guo, Q. Zhu, Y. Torimoto, and Q. Li, Chem. Commun. 5215 (2008).
[23] Z. Wang, Y. Pan, T. Dong, X. Zhu, T. Kan, L. Yuan, Y. Torimoto, M. Sadakata, and Q. Li, Appl. Catal. A **320**, 24 (2007).
[24] T. Hou, L. Yuan, T. Ye, L. Gong, J. Tu, M. Yamamoto, Y. Torimoto, and Q. Li, Int. J. Hydrogen Energy **34**, 9095 (2009).
[25] T. Ye, L. Yuan, Y. Chen, T. Kan, J. Tu, X. Zhu, Y. Torimoto, M. Yamamoto, and Q. Li, Catal. Lett. **127**, 323 (2009).
[26] J. Bao, Y. L. Fu, Z. H. Sun, and C. Gao, Chem. Commun. 746 (2003).
[27] Z. X. Wang, T. Dong, L. X. Yuan, T. Kan, X. F. Zhu, Y. Torimoto, M. Sadakata, and Q. X. Li, Energy Fuels **21**, 2421 (2007).
[28] W. Ma, E. L. Kugler, and D. B. Dadyburjor, Energy Fuels **21**, 1832 (2007).
[29] Y. Liu, F. Chen, S. Zhuang, J. Wang, and R. Ma, China, Pat.$CN_2$00710190420.0, (2007).
[30] G. P. Van Der Laan and A. A. C. M. Beenackers, Catal. Rev. Sci. Eng. **41**, 255 (1999).
[31] W. M. H. Sachtler and M. Ichikawa, J. Phys. Chem. **90**, 4752 (1986).
[32] M. E. Dry, Catal. Today **71**, 227 (2002).
[33] X. Huang, C. W. Curtis, and C. B. Roberts, Prepr. Pap. Am. Chem. Soc., Div. Fuel Chem. **47**, 150 (2002).
[34] Y. Liu, B. T. Teng, X. H. Guo, Y. Li, J. Chang, L. Tian, X. Hao, Y. Wang, H. W. Xiang, Y. Y. Xu, and Y. W. Li, J. Mol. Catal. A **272**, 182 (2007).
[35] Z. R. Li, Y. L. Fu, M. Jiang, Y. Xie, T. Hu, and T. Liu, Catal. Lett. **65**, 43 (2000).
[36] D. B. Li, C. Yang, W. H. Li, Y. H. Sun, and B. Zhong, Top. Catal. **32**, 233 (2005).
[37] T. Inui, T. Yamamoto, M. Inoue, H. Hara, T. Takeguchi, and J. B. Kim, Appl. Catal. A **186**, 395 (1999).
[38] X. M. Liu, G. Q. Lu, Z. F. Yan, and J. Beltramini, Ind. Eng. Chem. Res. **42**, 6518 (2003).
[39] P. Forzatti, E. Tronconi, and I. Pasquon, Catal. Rev. **33**, 109 (1991).
[40] T. Tatsumi, A. Muramatsu, and H. O. Tominaga, Chem. Lett. 685 (1984).
[41] J. G. Santiesteban, C. E. Bogdan, R. G. Herman, and K. Klier, *Proceedings of the 9th International Congress on Catalysis*, M. J. Phillips, M. Ternan, Eds., 561 (1988).
[42] K. J. Smith, R. G. Herman, and K. Klier, Chem. Eng. Sci. **45**, 2639 (1990).
[43] H. Schulz, Appl. Catal. A **186**, 3 (1999).
[44] R. Xu, C. Yang, W. Wei, W. H. Li, Y. H. Sun, and T. D. Hu, J. Mol. Catal. A **221**, 51 (2004).
[45] M. L. Xiang, D. B. Li, W. H. Li, B. Zhong, and Y. H. Sun, Catal. Commun. **8**, 513 (2007).
[46] N. Wang, K. G. Fang, M. G. Lin, D. Jiang, D. B. Li, and Y. H. Sun, Catal. Lett. **136**, 9 (2010).
[47] M. L. Xiang, D. B. Li, W. H. Li, B. Zhong, and Y. H. Sun, Catal. Commun. **8**, 88 (2007).
[48] J. P. Hindermann, G. J. Hutchings, and A. Kiennemann, Catal. Rev. **35**, 1 (1993).

DOI:10.1088/1674-0068/24/01/77-84